

多孔功能梯度压电纳米壳中波传播特性*

王鑫特, 刘娟, 胡彪, 张波, 沈火明

(西南交通大学 力学与航空航天学院, 成都 611756)

摘要: 基于非局部应变梯度理论, 探究了含孔隙的功能梯度压电陶瓷纳米壳中波传播特性. 利用 Hamilton 原理和一阶剪切理论推导了控制方程. 结合非局部应变梯度理论和谐波解得到了尺度依赖的特征方程. 数值讨论了尺度参数、波数、梯度指数、壳厚、孔隙率及电压对波传播特性的影响. 研究表明: 非局部参数和应变梯度参数对波传播频率的影响与波数密切相关, 在一定范围内波数越大, 尺度参数对频率的影响越大; 另外, 孔隙和梯度指数对频率具有耦合作用.

关键词: 压电纳米壳; 波动特性; 非局部应变梯度理论; 功能梯度

中图分类号: TB383; TB34 **文献标志码:** A **DOI:** 10.21656/1000-0887.440057

Wave Propagation in Functionally Graded Piezoelectric Nanoshells

WANG Xinte, LIU Juan, HU Biao, ZHANG Bo, SHEN Huoming
(School of Mechanics and Aerospace Engineering, Southwest Jiaotong University,
Chengdu 611756, P.R.China)

Abstract: The waves propagation characteristics in porous functionally graded piezoelectric nanoshells were investigated based on the nonlocal strain gradient theory. The governing equations were developed under Hamilton's principle and the 1st-order shear theory. The scale-dependent characteristic equations were obtained through combination of the nonlocal strain gradient theory and the harmonic solutions. The effects of the scale parameter, the wave number, the gradient index, the thickness, the porosity and the voltage on the wave propagation characteristics were discussed numerically. The results show that, the influences of the nonlocal parameter and the strain gradient parameter on the wave propagation frequency are closely related to the wave number, and the larger the wave number is in a certain range, the greater the influence of scale parameters on the frequency will be. In addition, the porosity and the gradient index have a coupling effect on the frequency.

Key words: piezoelectric nanoshell; wave propagation; nonlocal strain gradient theory; functionally graded

0 引 言

随着新型智能器件的高速发展, 开发各类多功能材料已成为一种趋势. 其中, 功能梯度压电材料 (func-

* 收稿日期: 2023-03-06; 修订日期: 2023-05-03

基金项目: 国家自然科学基金 (11502218)

作者简介: 王鑫特 (1998—), 男, 硕士 (E-mail: 15833215871@163.com);

刘娟 (1986—), 女, 副教授, 博士 (通讯作者. E-mail: lj187@swjtu.edu.cn).

引用格式: 王鑫特, 刘娟, 胡彪, 张波, 沈火明. 多孔功能梯度压电纳米壳中波传播特性 [J]. 应用数学和力学, 2024, 45(2): 197-207.

tionally graded pizeoelectric material, FGPM)是采用先进的材料复合技术将两种或多种不同材料耦合而成的非均质材料^[1].FGPM的构成要素(组份、组织、显微气孔率等)随空间位置呈梯度性连续变化,能充分减少和克服组份材料结合部位界面性能的不匹配因素,具有良好的抗变形能力、机电转换性及耐腐蚀性^[2-4].在FGPM制造过程中可通过调控两种或两种以上材料组分的体积分数、孔隙率等参数来设计材料性能,以满足工程结构特定的功能要求.随着智能器件逐渐向微型化方向发展,FGPM的应用范围逐渐延伸至纳机电系统领域.纳机电系统中承载构件可以简化为特征尺度处于纳米量级的梁、板、壳等结构,典型应用为纳米谐振器、纳米传感器、纳米执行器、纳米开关等.

随着构件特征尺寸减小至纳米尺度,原子之间长程作用力会显著增加,尺度效应变得不可忽略.分子动力学模拟表明,经典连续介质力学理论所预测的纳米结构振动频率与实测结果相差10%~30%^[5].因此,寻找和发展适应于纳米力学研究的新途径和新方法,是当前连续力学的研究热点之一^[6].由Eringen^[7]提出的非局部弹性理论在纳米力学研究中扮演着重要角色,非局部连续力学将分子间作用力是长程力的思想引入到传统连续介质力学中,认为连续体内某一点的应力不仅取决于该点的应变,还是连续体内所有点的应变及应变梯度的函数.非局部理论被诸多学者证明能成功地预测软化效应^[8-10].然而Kuang等^[11]研究了含流体的双壁碳纳米管的非线性振动,表明非局部弹性模型无法预测材料可能存在的刚度硬化效应.而且在不同金属材料的微纳米压痕实验中^[12-13],同样观察到了非局部理论无法解释的微尺度下材料强度比常规尺度下材料强度显著提高的现象,而应变梯度假设则是将连续体中的每一个物质点看作含有高阶应变的胞元,据此引入长度尺度参数来表征其对结构力学性能的影响,该参数可合理地预测结构中的刚度硬化效应^[14].Lim等^[15]基于非局部理论并结合应变梯度假设,提出了新的非局部应变梯度理论.该理论考虑了应变梯度的非局部效应,也考虑了材料物质点处高阶应力梯度的非局部效应.Lim等将该理论应用于纳米梁和碳纳米管中的波传播分析中,揭示了关于晶格动力学和波传播实验的一些新发现.Ma等^[16]通过两种非局部应变梯度壳理论,研究了磁电弹性纳米壳中的波传播特性,总结了电-磁-机械荷载与截止波数的关系.Wang和他的同事^[17-19]利用非局部应变梯度理论,对功能分级纳米板在弯曲、屈曲和轴向运动时的振动特性和稳定性进行了系统研究,并且在这些机械运动中都观察到了刚度软化和硬化机制.此外,不少学者也利用非局部应变梯度理论探究了FGPM纳米结构的动态特性^[20-21].然而,以上研究对孔隙作用下FGPM纳米壳的波动特性关注较少.

本文采用基于非局部应变梯度理论的一阶剪切壳模型研究了多孔FGPM纳米材料的波传播特性.根据Hamilton原理推导了结构的非局部运动微分方程,进而通过数值分析研究了尺度参数、几何参数、内部结构参数、外部电压等参数对波传播特性的影响.

1 多孔FGPM纳米壳的动力学建模

1.1 非局部应变梯度理论

由Lim等建立的非局部应变梯度理论综合考虑了应力场与高阶应力场的非局部性.其应力场可表示为^[22-23]

$$t_{ij} = \sigma_{ij}^{(1)} - \nabla \sigma_{ij}^{(2)}, \quad (1)$$

其中, $\sigma_{ij}^{(1)}$ 是经典非局部应力, $\sigma_{ij}^{(2)}$ 是高阶非局部应力, ∇ 是Laplace算子.该理论通过引入两个尺度参数,同时涉及了应变和应变梯度的非局部效应,式(1)中的两个应力可由尺度参数及对应应变表示为^[24]

$$\sigma_{ij}^{(1)} = \int_0^L \alpha_0(|x-x'|, e_0 a) c_{ijkl} \varepsilon'_{kl}(x') dx', \quad (2)$$

$$\sigma_{ij}^{(2)} = l^2 \int_0^L \alpha_1(|x-x'|, e_1 a) c_{ijkl} \varepsilon'_{kl,x}(x') dx', \quad (3)$$

式中, l 是表征高阶应变梯度效应的材料特征长度参数, α_0 与 α_1 是非局部核函数, $e_0 a$ 和 $e_1 a$ 是表征非局部效应的非局部参数, c_{ijkl} 是弹性系数, ε'_{kl} 和 $\varepsilon'_{kl,x}$ 分别是应变和应变梯度.将式(2)、(3)代入式(1)中,引入Laplace算子 ∇^2 ,可得到一种简化应力和非局部应力的关系:

$$[1 - (e_1 a)^2 \nabla^2][1 - (e_0 a)^2 \nabla^2] \sigma_{ij} = [(1 - (e_1 a)^2 \nabla^2) - l^2 \nabla^2 (1 - (e_0 a)^2 \nabla^2)] c_{ijkl} \varepsilon_{kl}. \quad (4)$$

经典非局部应变梯度理论假设 $e_0 = e_1$,并忽略高阶项 $O(\nabla^2)$,即可得到基于该理论的本构方程为

$$[1 - \mu \nabla^2] \sigma_{ij} = (1 - \eta \nabla^2) c_{ijkl} \varepsilon_{kl}, \quad (5)$$

其中, $\mu = (e_0 a)^2$, $\eta = l^2$. 在电场的影响下, FGPM 纳米壳结构的矩阵形式本构方程可以定义为

$$(1 - \mu \nabla^2) \begin{Bmatrix} \sigma_{xx} \\ \sigma_{\theta\theta} \\ \sigma_{x\theta} \\ \sigma_{\theta z} \\ \sigma_{xz} \end{Bmatrix} = (1 - \eta \nabla^2) \begin{Bmatrix} \tilde{c}_{11} & \tilde{c}_{12} & 0 & 0 & 0 \\ \tilde{c}_{12} & \tilde{c}_{22} & 0 & 0 & 0 \\ 0 & 0 & \tilde{c}_{66} & 0 & 0 \\ 0 & 0 & 0 & \tilde{c}_{44} & 0 \\ 0 & 0 & 0 & 0 & \tilde{c}_{55} \end{Bmatrix} \begin{Bmatrix} \varepsilon_{xx} \\ \varepsilon_{\theta\theta} \\ \gamma_{x\theta} \\ \gamma_{\theta z} \\ \gamma_{xz} \end{Bmatrix} - \begin{Bmatrix} 0 & 0 & \tilde{e}_{31} \\ 0 & 0 & \tilde{e}_{32} \\ 0 & 0 & 0 \\ 0 & \tilde{e}_{24} & 0 \\ \tilde{e}_{15} & 0 & 0 \end{Bmatrix} \begin{Bmatrix} E_x \\ E_\theta \\ E_z \end{Bmatrix}, \quad (6)$$

$$(1 - \mu \nabla^2) \begin{Bmatrix} D_x \\ D_\theta \\ D_z \end{Bmatrix} = (1 - \eta \nabla^2) \begin{Bmatrix} \tilde{e}_{15} \gamma_{xz} + \tilde{s}_{11} E_x \\ \tilde{e}_{24} \gamma_{\theta z} + \tilde{s}_{22} E_\theta \\ \tilde{e}_{31} \varepsilon_{xx} + \tilde{e}_{32} \varepsilon_{\theta\theta} + \tilde{s}_{33} E_z \end{Bmatrix}, \quad (7)$$

其中, $\tilde{c}_{ij}, \tilde{e}_{ij}, \tilde{s}_{ij}$ 为材料的弹性系数、压电系数及介电系数, E_i 为纳米壳任意一点处 i 方向的电位移。

1.2 多孔 FGPM 纳米壳的几何描述

本文采用由压电陶瓷 PZT-4 与 PZT-5H 耦合组成的多孔 FGPM 纳米壳模型, 如图 1 所示。壳长度为 L , 半径为 R , 厚度为 h , 图中 $U(x, \theta, z, t), V(x, \theta, z, t)$ 和 $W(x, \theta, z, t)$ 是壳上任意一点处在 x, θ, z 三个方向上的位移。壳内部含有的孔隙分布形式可看做是均匀分布, FGPM 纳米壳的材料常数^[25]可表示为

$$P(z) = (P_4 - P_{5H}) \left(\frac{z}{h} + \frac{1}{2} \right)^N + P_{5H} - (P_4 + P_{5H}) \frac{\alpha}{2}, \quad (8)$$

其中, z 为纳米壳中任意一点到中表面的垂直距离, 参数 $N \in [0, \infty)$ 表示幂律指数, 即功能梯度指数, 参数 α 为孔隙率。为了满足 Maxwell 方程, FGPM 纳米壳外部沿厚度方向分布的电势定义为^[26]

$$\tilde{\Phi}(x, \theta, z, t) = -\cos(\beta z) \Phi(x, \theta, t) + \frac{2zV_0}{h}, \quad (9)$$

其中, $\beta = \pi/h$ 为一个线性常数, $\Phi(x, \theta, t)$ 表示壳平面上分布的电势, V_0 代表初始的外加电压。

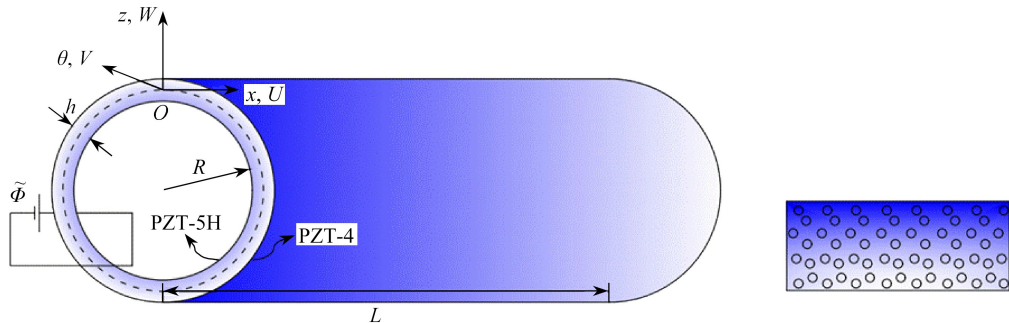


图 1 多孔 FGPM 纳米壳的模型示意图

Fig. 1 The geometric model for the porous FGPM nanoshell

利用一阶剪切变形壳模型方程分析位移场^[27], 得到壳中任意一点处的位移分量为

$$\begin{Bmatrix} u(x, \theta, z, t) \\ v(x, \theta, z, t) \\ w(x, \theta, z, t) \end{Bmatrix} = \begin{Bmatrix} U(x, \theta, t) \\ V(x, \theta, t) \\ W(x, \theta, t) \end{Bmatrix} + z \begin{Bmatrix} \psi_x(x, \theta, t) \\ \psi_\theta(x, \theta, t) \\ 0 \end{Bmatrix}. \quad (10)$$

FGPM 纳米壳任意一点处的电位移为

$$E_x = -\tilde{\Phi}_{,x} = \cos(\beta z) \frac{\partial \Phi}{\partial x}, \quad (11)$$

$$E_\theta = -\frac{1}{R+z} \tilde{\Phi}_{,\theta} = \frac{\cos(\beta z)}{R+z} \frac{\partial \Phi}{\partial \theta}, \quad (12)$$

$$E_z = -\tilde{\Phi}_{,z} = -\beta \sin(\beta z) \Phi - \frac{2V_0}{h}. \quad (13)$$

1.3 多孔 FGPM 纳米壳的运动微分方程

FGPM 纳米壳上各个点处的动能 Π_K 为

$$\Pi_K = \frac{1}{2} \int_v \rho \left[\left(\frac{\partial u}{\partial t} \right)^2 + \left(\frac{\partial v}{\partial t} \right)^2 + \left(\frac{\partial w}{\partial t} \right)^2 \right] dv. \quad (14)$$

模型应变能 Π_S 为

$$\Pi_S = \frac{1}{2} \int_v (\sigma_{ij} \varepsilon_{kl} - D_i E_k) dv. \quad (15)$$

轴向和环向电场力对 FGPM 纳米壳做功为

$$\Pi_F = \frac{1}{2} \int_s \left[N_{Ex} \left(\frac{\partial W}{\partial x} \right)^2 + N_{E\theta} \left(\frac{\partial W}{R \partial \theta} \right)^2 \right] ds. \quad (16)$$

将式(14)–(16)代入 Hamilton 原理

$$\int_0^t (\delta \Pi_K - \delta \Pi_S - \delta \Pi_F) dt = 0, \quad (17)$$

可得如下控制微分方程:

$$\frac{\partial N_x}{\partial x} + \frac{1}{R} \frac{\partial N_{x\theta}}{\partial \theta} = I_0 \frac{\partial^2 U}{\partial t^2} + I_1 \frac{\partial^2 \psi_x}{\partial t^2}, \quad (18)$$

$$\frac{1}{R} \frac{\partial N_\theta}{\partial \theta} + \frac{\partial N_{x\theta}}{\partial x} + \frac{N_{\theta z}}{R} = I_0 \frac{\partial^2 V}{\partial t^2} + I_1 \frac{\partial^2 \psi_\theta}{\partial t^2}, \quad (19)$$

$$\frac{\partial N_{xz}}{\partial x} + \frac{1}{R} \frac{\partial N_{\theta z}}{\partial \theta} - \frac{N_\theta}{R} - N_{Ex} \frac{\partial^2 W}{\partial x^2} - N_{E\theta} \frac{1}{R^2} \frac{\partial^2 W}{\partial \theta^2} = I_0 \frac{\partial^2 W}{\partial t^2}, \quad (20)$$

$$\frac{\partial M_x}{\partial x} + \frac{1}{R} \frac{\partial M_{x\theta}}{\partial \theta} - N_{xz} = I_1 \frac{\partial^2 U}{\partial t^2} + I_2 \frac{\partial^2 \psi_x}{\partial t^2}, \quad (21)$$

$$\frac{1}{R} \frac{\partial M_\theta}{\partial \theta} + \frac{\partial M_{x\theta}}{\partial x} - N_{\theta z} = I_1 \frac{\partial^2 V}{\partial t^2} + I_2 \frac{\partial^2 \psi_\theta}{\partial t^2}, \quad (22)$$

$$\int_l \left(\cos(\beta z) \frac{\partial D_x}{\partial x} + \frac{\cos(\beta z)}{R+z} \frac{\partial D_\theta}{\partial \theta} + D_z \beta \sin(\beta z) \right) dl = 0, \quad (23)$$

其中

$$(I_0, I_1, I_2) = \int_{-h/2}^{h/2} \rho(1, z, z^2) dz, \quad (24)$$

$$(N_{Ex}, N_{E\theta}) = -2(\tilde{\varepsilon}_{31}, \tilde{\varepsilon}_{32}) V_0, \quad (25)$$

$$(N_x, N_\theta, N_{x\theta}, N_{xz}, N_{\theta z}) = \int_{-h/2}^{h/2} (\sigma_{xx}, \sigma_{\theta\theta}, \sigma_{x\theta}, \sigma_{\theta z}, \sigma_{xz}) dz, \quad (26)$$

$$(M_x, M_\theta, M_{x\theta}) = \int_{-h/2}^{h/2} (\sigma_{xx}, \sigma_{\theta\theta}, \sigma_{x\theta}) z dz. \quad (27)$$

将非局部应变梯度本构方程(4)沿纳米壳径向进行积分,并将所得力和力矩表达式代入控制方程(15)–(20)中,可得位移形式的结构运动微分方程如下:

$$\Gamma_\eta \left(A_{11} \frac{\partial^2 U}{\partial x^2} + \frac{A_{66}}{R^2} \frac{\partial^2 U}{\partial \theta^2} + \frac{A_{12} + A_{66}}{R} \frac{\partial^2 V}{\partial x \partial \theta} + \frac{A_{12}}{R} \frac{\partial W}{\partial x} + B_{11} \frac{\partial^2 \psi_x}{\partial x^2} + \frac{B_{66}}{R^2} \frac{\partial^2 \psi_x}{\partial \theta^2} + \frac{B_{12} + B_{66}}{R} \frac{\partial^2 \psi_\theta}{\partial x \partial \theta} + F_{31} \frac{\partial \Phi}{\partial x} \right) = \Gamma_\mu \left(I_0 \frac{\partial^2 U}{\partial t^2} + I_1 \frac{\partial^2 \psi_x}{\partial t^2} \right), \quad (28)$$

$$\Gamma_\eta \left(\frac{A_{12} + A_{66}}{R} \frac{\partial^2 U}{\partial x \partial \theta} + \frac{A_{22}}{R^2} \frac{\partial^2 V}{\partial \theta^2} + A_{66} \frac{\partial^2 V}{\partial x^2} - \frac{A_{44}}{R^2} V + \frac{A_{22} + A_{44}}{R^2} \frac{\partial W}{\partial \theta} + \frac{B_{12} + B_{66}}{R} \frac{\partial^2 \psi_x}{\partial x \partial \theta} + \frac{B_{22}}{R^2} \frac{\partial^2 \psi_\theta}{\partial \theta^2} + B_{66} \frac{\partial^2 \psi_\theta}{\partial x^2} + \frac{A_{44}}{R} \psi_\theta + \frac{F_{32} - E_{24}}{R} \frac{\partial \Phi}{\partial \theta} \right) = \Gamma_\mu \left(I_0 \frac{\partial^2 V}{\partial t^2} + I_1 \frac{\partial^2 \psi_\theta}{\partial t^2} \right), \quad (29)$$

$$\Gamma_{\eta} \left[-\frac{A_{12}}{R} \frac{\partial U}{\partial x} - \frac{A_{22} + A_{44}}{R^2} \frac{\partial V}{\partial \theta} + A_{55} \frac{\partial^2 W}{\partial x^2} + \frac{A_{44}}{R^2} \frac{\partial^2 W}{\partial \theta^2} - \frac{A_{22}}{R^2} W + \left(A_{55} - \frac{B_{12}}{R} \right) \frac{\partial \psi_x}{\partial x} + \left(\frac{A_{44}}{R} - \frac{B_{22}}{R^2} \right) \frac{\partial \psi_{\theta}}{\partial \theta} - E_{15} \frac{\partial^2 \Phi}{\partial x^2} - \frac{E_{24}}{R} \frac{\partial^2 \Phi}{\partial \theta^2} - \frac{F_{32}}{R} \Phi \right] = \Gamma_{\mu} \left(N_{Ex} \frac{\partial^2 W}{\partial x^2} + \frac{N_{E\theta}}{R^2} \frac{\partial^2 W}{\partial \theta^2} + I_0 \frac{\partial^2 W}{\partial t^2} \right), \quad (30)$$

$$\Gamma_{\eta} \left[B_{11} \frac{\partial^2 U}{\partial x^2} + \frac{B_{66}}{R^2} \frac{\partial^2 U}{\partial \theta^2} + \frac{B_{12} + B_{66}}{R} \frac{\partial^2 V}{\partial x \partial \theta} + \left(\frac{B_{12}}{R} - A_{55} \right) \frac{\partial W}{\partial x} + D_{11} \frac{\partial^2 \psi_x}{\partial x^2} + \frac{D_{66}}{R^2} \frac{\partial^2 \psi_x}{\partial \theta^2} - A_{55} \psi_x + \frac{D_{12} + D_{66}}{R} \frac{\partial^2 \psi_{\theta}}{\partial x \partial \theta} + (E_{31} + E_{15}) \frac{\partial \Phi}{\partial x} \right] = \Gamma_{\mu} \left(I_1 \frac{\partial^2 U}{\partial t^2} + I_2 \frac{\partial^2 \psi_x}{\partial t^2} \right), \quad (31)$$

$$\Gamma_{\eta} \left[\frac{B_{12} + B_{66}}{R} \frac{\partial^2 U}{\partial x \partial \theta} + \frac{B_{22}}{R^2} \frac{\partial^2 V}{\partial \theta^2} + B_{66} \frac{\partial^2 V}{\partial x^2} + A_{44} \frac{V}{R} + \left(\frac{B_{22}}{R^2} - \frac{A_{44}}{R} \right) \frac{\partial W}{\partial \theta} + \frac{D_{66} + D_{12}}{R} \frac{\partial^2 \psi_x}{\partial x \partial \theta} + D_{66} \frac{\partial^2 \psi_{\theta}}{\partial x^2} + \frac{D_{22}}{R^2} \frac{\partial^2 \psi_{\theta}}{\partial \theta^2} - A_{44} \psi_{\theta} + \left(\frac{E_{32}}{R} + E_{24} \right) \frac{\partial \Phi}{\partial \theta} \right] = \Gamma_{\mu} \left(I_1 \frac{\partial^2 V}{\partial t^2} + I_2 \frac{\partial^2 \psi_{\theta}}{\partial t^2} \right), \quad (32)$$

$$\Gamma_{\eta} \left[F_{31} \frac{\partial U}{\partial x} + \frac{F_{32} - E_{24}}{R} \frac{\partial V}{\partial \theta} + E_{15} \frac{\partial^2 W}{\partial x^2} + \frac{E_{24}}{R} \frac{\partial^2 W}{\partial \theta^2} + \frac{F_{32}}{R} W + (E_{15} + E_{31}) \frac{\partial \psi_x}{\partial x} + \left(\frac{E_{32}}{R} + E_{24} \right) \frac{\partial \psi_{\theta}}{\partial \theta} + X_{11} \frac{\partial^2 \Phi}{\partial x^2} + X_{22} \frac{\partial^2 \Phi}{\partial \theta^2} - X_{33} \Phi \right] = 0, \quad (33)$$

其中, $\Gamma_{\mu} = (1 - \mu \nabla^2)$, $\Gamma_{\eta} = (1 - \eta \nabla^2)$.

2 多孔 FGPM 纳米壳波传播问题的求解

针对 FGPM 纳米壳内每一点处波传播响应的模拟问题,引入壳结构波传播通解^[28]:

$$\begin{Bmatrix} U(x, \theta, t) \\ V(x, \theta, t) \\ W(x, \theta, t) \\ \psi_x(x, \theta, t) \\ \psi_{\theta}(x, \theta, t) \\ \Phi(x, \theta, t) \end{Bmatrix} = \begin{Bmatrix} U_m \\ V_m \\ W_m \\ \psi_{xm} \\ \psi_{\theta m} \\ \Phi_m \end{Bmatrix} \exp[i(kx + n\theta - \omega t)], \quad (34)$$

其中, $U_m, V_m, W_m, \psi_{xm}, \psi_{\theta m}$ 分别表示纳米壳各个点处波传播的位移与转角的幅值, Φ_m 表示电势幅值, i 为虚数单位, k 和 n 表示波传播时沿着 x 方向产生的纵向波数和沿着转角 θ 方向产生的周向波数. 将通解方程 (34) 代入运动微分方程 (28) — (33) 中, 即可得到 FGPM 纳米壳的波传播特征方程为

$$(\mathbf{L}_{6 \times 6} - \omega^2 \mathbf{H}_{6 \times 6}) \begin{Bmatrix} U_m \\ V_m \\ W_m \\ \psi_{xm} \\ \psi_{\theta m} \\ \Phi_m \end{Bmatrix} = \mathbf{0}, \quad (35)$$

其中, $\mathbf{L}_{6 \times 6}$ 与 $\mathbf{H}_{6 \times 6}$ 分别为刚度系数矩阵以及质量系数矩阵, 角频率 ω 的值可由系数矩阵的行列式等于零求得, 而波传播频率 f 的值可根据 f 与 ω 的关系式得到:

$$f = \frac{\omega}{2\pi}. \quad (36)$$

3 数值结果及分析

本节通过求解特征方程(32),研究了波数、尺度参数、几何参数、外部电势、孔隙率以及功能梯度指数对图1所示FGPM圆柱形纳米壳波传播特性的影响,两种材料参数如表1所示^[29].

表1 FGPM的材料特性数值

Table 1 Material properties of the FGPM

material	unit	PZT-4	PZT-5H
elastic modulus	GPa	$c_{11} = 139, c_{12} = 77.8, c_{13} = 74,$	$c_{11} = 126, c_{12} = 79.1, c_{13} = 83.9,$
		$c_{22} = 139, c_{23} = 74, c_{33} = 115,$	$c_{22} = 126, c_{23} = 83.9, c_{33} = 117,$
		$c_{44} = 25.6, c_{55} = 25.6, c_{66} = 30.6$	$c_{44} = 23, c_{55} = 23, c_{66} = 23.5$
piezoelectric modulus	C/m ²	$e_{31} = -5.2, e_{32} = -5.2, e_{33} = 15.1,$	$e_{31} = -6.5, e_{32} = -6.5, e_{33} = 23.3,$
		$e_{15} = 12.7, e_{24} = 12.7$	$e_{15} = 17, e_{24} = 17$
dielectric modulus	C/(V·m)	$s_{11} = 5.841 \times 10^{-9}, s_{33} = 7.124 \times 10^{-9}$	$s_{11} = 1.505 \times 10^{-8}, s_{33} = 1.302 \times 10^{-8}$
mass density	kg/m ³	$\rho = 7500$	$\rho = 7500$

3.1 有效性验证

为了检验理论模型的正确性,将FGPM纳米壳的结果和磁电弹纳米壳的结果进行验证.基于非局部理论将本文得到的波传播频散关系与Ma等^[16]的结果(文献[16]中的图3(a))进行对比(图2).可以看出,本研究的结果与Ma等^[16]的结果良好吻合,验证了本研究的有效性.

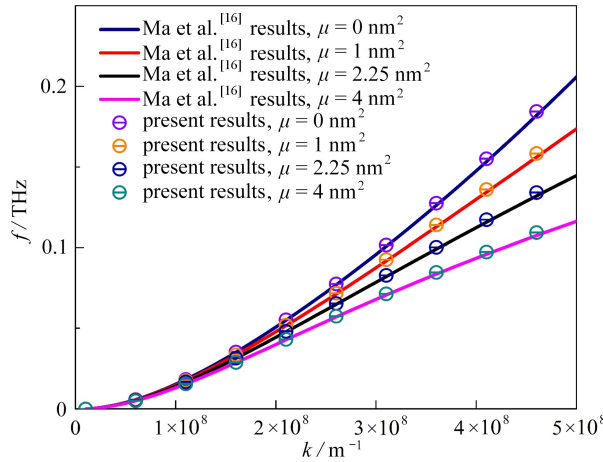


图2 退化验证 ($\eta = 1 \text{ nm}^2$)

Fig. 2 Comparison of frequency dispersion results ($\eta = 1 \text{ nm}^2$)

注 为了解释图中的颜色,读者可以参考本文的电子网页版本,后同.

3.2 数值讨论

表2表示前三阶固有频率(f_1, f_2, f_3)与纵向波数 k 和周向波数 n 的关系.从表中可以看出三阶频率随着纵向及周向波数的增加而增加,且两方向波数对频率的增加影响呈现互补效果.本文后续工作主要分析探究纳米壳中波传播的纵向波数 k 对基频 f 的影响.

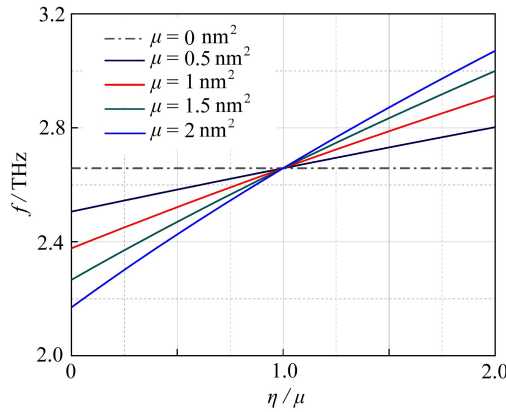
图3显示了在不同波数 k 下,两个尺度参数间比值 η/μ 的变化对FGPM纳米壳波传播频率 f 的影响.图中 $n = 1, h = 20 \text{ nm}, R = 200 \text{ nm}, \alpha = 0.2, N = 2, \Phi_0 = 5 \text{ V}$.从图中可以看出,整体上,当 $\eta/\mu < 1$ 时,非局部应变梯度理论对应的频率都小于通过经典弹性理论得到的频率,这是因为非局部效应占主导地位时,会使得壳的刚度减弱,呈现软化效应.相反地,当 $\eta/\mu > 1$ 时,非局部应变梯度理论获得的频率都大于通过经典弹性理论得到的频率,此时占主导地位的应变梯度效应使得壳的刚度增强,呈现硬化效应.当 $\eta/\mu = 1$ 时,非局部应变梯度理论和经典弹性理论得到的频率是等价的,说明两种类型的尺寸依赖效应会相互抵消.此外,固定长度尺度参数 η 不变,在不同波数下同等程度的改变非局部参数 μ ,发现当波数较大时导致的频移大于波

数较小时对应的频移.同理,固定 μ 不变时, η 对 f 的影响也随着 k 的增大而增大.这表明由非局部参数引起的软化效应和由应变梯度参数引起的硬化效应在波数较大时更加明显,在波数较小时较为微弱.所以对于纳米壳尺度效应的频散特性研究不仅需要考虑到尺度效应的作用,也需要关注波数的影响.

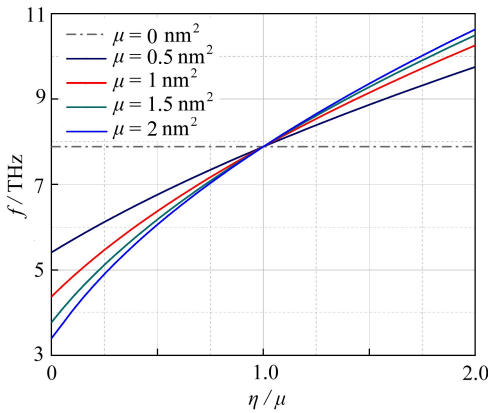
表 2 前三阶固有频率 (f_1, f_2, f_3) 与纵向波数 k 和周向波数 n 的关系

Table 2 The 1st 3 orders of frequencies vs. longitudinal and circumferential wave numbers

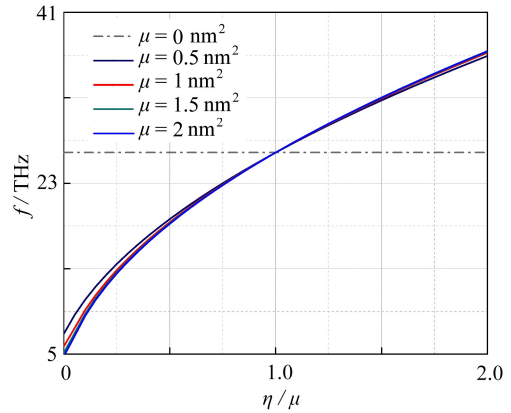
n	k/m^{-1}	f_1/THz	f_2/THz	f_3/THz
1	1×10^8	0.727 8	1.407 4	2.375 5
	5×10^8	2.881 4	3.119 8	3.219 8
	1×10^9	6.448 6	7.129 6	7.514 7
10	1×10^8	0.773 5	1.330 0	2.242 7
	5×10^8	2.929 7	3.175 6	3.275 2
	1×10^9	6.457 7	7.140 8	7.526 7
100	1×10^8	2.973 8	3.235 4	3.336 7
	5×10^8	4.301 9	4.838 0	4.916 2
	1×10^9	7.327 1	8.172 2	8.646 4



(a) $k = 5 \times 10^8 \text{ m}^{-1}$



(b) $k = 1 \times 10^9 \text{ m}^{-1}$



(c) $k = 5 \times 10^9 \text{ m}^{-1}$

图 3 基于不同波数,变化的 η/μ 比值对 FGPM 纳米壳波传播频率的影响

Fig. 3 Frequencies vs. η/μ values for different wave numbers of the FGPM nanoshell

图 4 为基于非局部应变梯度理论,在不同波数 k 下,变化的功能梯度指数 N 对 FGPM 纳米壳波传播频率的影响.图中 $n = 1, R = 200 \text{ nm}, \alpha = 0.2, N = 2, \Phi_0 = 2 \text{ V}$.在图 4 中也可以观察到图 3 中的类似现象.这是由于当 $\eta < \mu$ 和 $\eta > \mu$ 时,非局部参数的软化效应和应变梯度参数的硬化效应得到了体现.特别地,当两个参数取值不同但比值相同时,其对应的 $f-N$ 曲线在波数较小时间距很大,而在波数较大时近似重合.这也证明

了纳米结构中的波传播行为研究需要考虑尺度效应和波数的共同作用.此外,还可以看出,波传播频率 f 随着功能梯度指数 N 的增加而减小.这是因为在由PZT-4与PZT-5H耦合组成的FGPM纳米壳中,当 N 增大时,材料的整体性能 P 会更接近于 P_{5H} ,而 P_{5H} 的弹性模量小于 P_4 ,从而整个纳米壳的弹性模量会减小,与之相对应的频率也会减小.且通过对比发现,频率 f 受梯度指数 N 的影响程度随着波数的增加而增加,也即纳米壳频率受到功能梯度指数和波数的耦合作用.

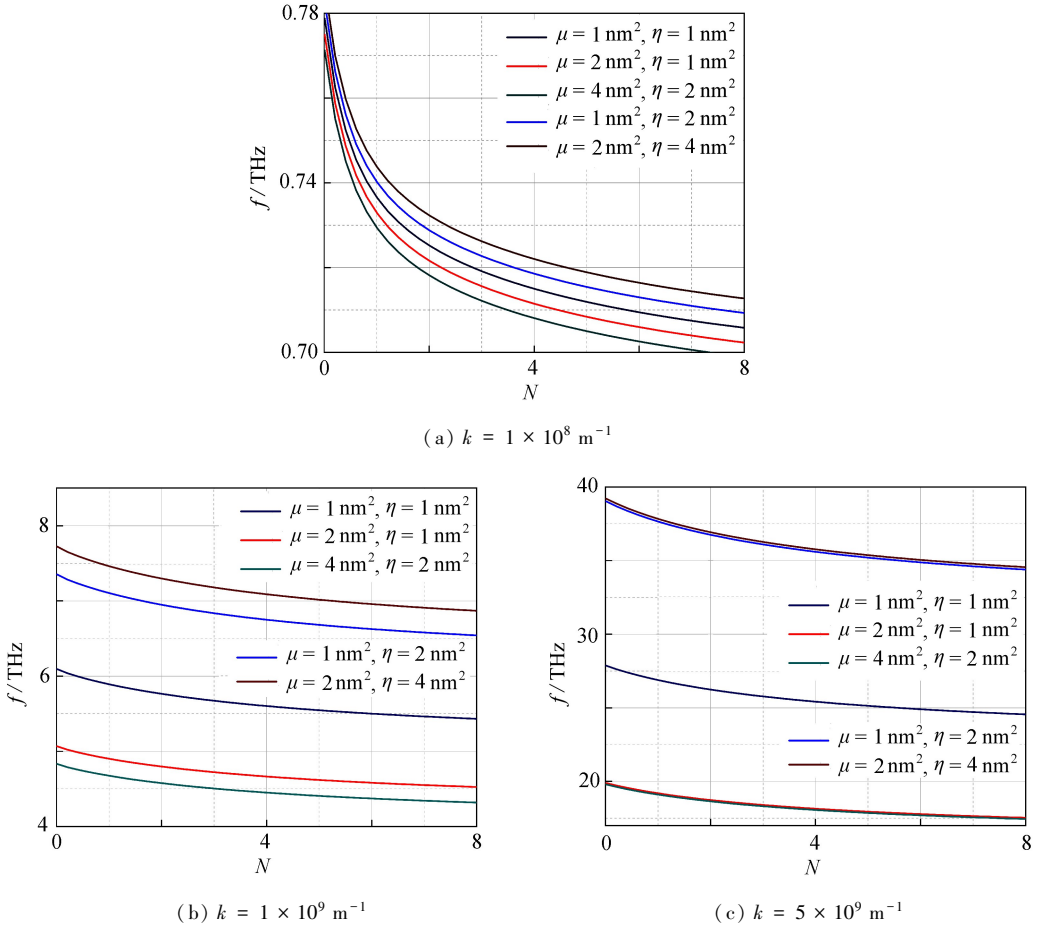


图4 基于不同波数,变化的尺度参数和功能梯度指数对FGPM纳米壳波传播频率的影响

Fig. 4 Frequencies vs. scale parameters and FG indexes for different wave numbers of the FGPM nanoshell

图5探讨了对于不同的壳厚 h ,FGPM纳米壳的频率 f 与功能梯度指数 N 间的关系.图中 $\mu = 1 \text{ nm}^2$, $\eta = 2 \text{ nm}^2$, $n = 1$, $k = 5 \times 10^8 \text{ m}^{-1}$, $R = 200 \text{ nm}$, $\alpha = 0.2$, $\Phi_0 = 2 \text{ V}$.从图中可以看出,波传播频率 f 随着壳厚 h 的增加而降低,且在壳厚 h 越小时,频率对壳厚 h 变化越敏感.这是因为壳厚变大会导致结构刚度和质量的同时增加,而对于由PZT-4和PZT-5H复合而成的FGPM纳米壳,在一定范围内,由质量增加导致波传播频率的降低程度比由刚度增加导致频率的增大程度更大.因此,更大的厚度会导致更低的频率,而且这种影响程度随着壳厚的减小而更加显著.

图6中给出了孔隙率 α 和功能梯度指数 N 对FGPM纳米壳波传播频率 f 的影响.图中 $\mu = 1 \text{ nm}^2$, $\eta = 2 \text{ nm}^2$, $n = 1$, $k = 5 \times 10^8 \text{ m}^{-1}$, $h = 20 \text{ nm}$, $R = 200 \text{ nm}$, $\Phi_0 = 2 \text{ V}$.由图可知,孔隙率 α 和功能梯度指数 N 对波传播频率有耦合影响,当 N 从0开始小范围内增加时,纳米壳的频率 f 会随着孔隙率 α 的增加而增加.当 $N > 3.6$ 时,规律则会相反,即频率 f 随着孔隙率 α 的增加而减少.这是因为孔隙率对材料刚度的影响与此时的功能梯度指数有关.当 $N < 3.6$ 时, N 减小,材料的刚度在增加,而 α 的增大会减小材料的刚度,但此时 N 较小,刚度较大的材料 P_4 占比很大,即在这一耦合作用中,由 N 减小导致增加的材料刚度大于由 α 增大而减小的材料刚度,所以频率会增大.当 $N > 3.6$ 时, N 与 α 的增加同时导致材料刚度的减少,从而导致频率快速减小.这说明对于两种材料耦合组成的多孔FGPM,可以通过改变结构的孔隙率和功能梯度指数来控制波在该

结构中的传播。

图 7 为在不同外加电势作用下,FGPM 纳米壳的频率与功能梯度指数的函数关系图。图中 $\mu = 1 \text{ nm}^2$, $\eta = 2 \text{ nm}^2$, $n = 1$, $k = 5 \times 10^8 \text{ m}^{-1}$, $\alpha = 0.2$, $h = 20 \text{ nm}$, $R = 200 \text{ nm}$ 。由图可知,波传播频率会随着正向电压增大而减小,而随反向电压的增大而增大。这是由于在对模型结构施加正/反向电势时,会在结构的轴向和周向产生压/拉力,使得结构的刚度发生软/硬化效应,从而减少/增加波传播频率。特别地,从图中可看出,频率对反向电压变化的敏感度大于对正向电压的敏感度。此外,还可观察到频率受正向与反向电压的影响均随着功能梯度指数的增加而变得明显。这是因为 N 越大,材料 P_{5H} 占比越多,而 P_{5H} 的压电系数大于 P_4 ,与之相对应的电压对频率的影响程度也会增加。

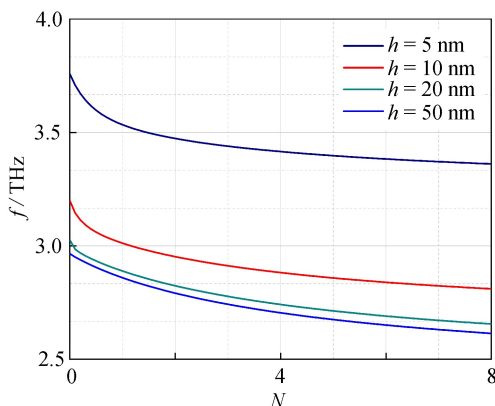


图 5 不同壳厚下 FGPM 纳米壳的频率与功能梯度指数的关系

Fig. 5 Frequencies vs. FG indexes for different thicknesses of the FGPM nanoshell

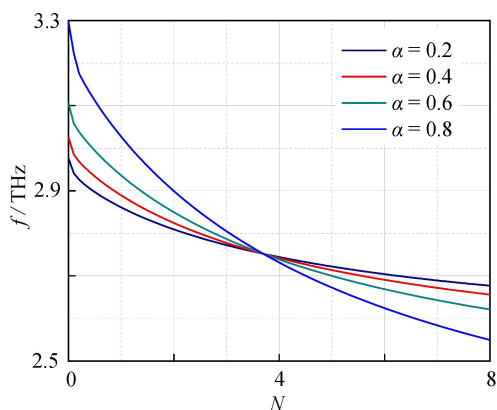


图 6 不同孔隙率下 FGPM 纳米壳的频率与功能梯度指数的关系

Fig. 6 Frequencies vs. FG indexes for different porosities of the FGPM nanoshell

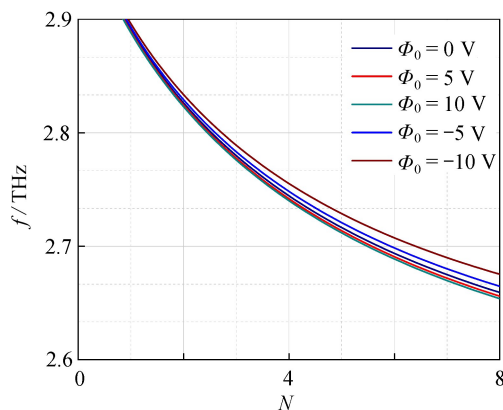


图 7 不同外电压作用下 FGPM 纳米壳的频率与功能梯度指数的关系

Fig. 7 Frequencies vs. FG indexes for different electric voltages of the FGPM nanoshell

4 结 论

本文基于非局部应变梯度理论建立了多孔 FGPM 纳米壳的尺度依赖模型,数值分析了尺度参数、梯度指数、孔隙率、壳厚和电压对波传播频率的影响,主要结论如下:

- 1) 当尺度参数间比值 $\eta/\mu < 1$ 时,会使材料刚度呈现软化效应,而 $\eta/\mu > 1$ 时,则呈现硬化效应,另外,增大波数或减小壳厚会加剧尺度效应;
- 2) 增大功能梯度指数或纳米壳厚度会减小波传播频率,其中,波数越大,梯度指数的影响程度越大;
- 3) 孔隙和功能梯度指数对频率具有耦合作用,功能梯度指数较小时,功能梯度指数和孔隙对频率的作用总体表现为增强,反之表现为降低;

4) 对结构施加正向电压,波传播频率会减小,施加反向电压,频率会增大,且电压对频率的影响程度随着功能梯度指数的增加而增加。

参考文献(References):

- [1] 夏巍,冯浩成.热过屈曲功能梯度壁板的气动弹性颤振[J].力学学报,2016,48(3):609-614.(XIA Wei, FENG Haocheng. Aeroelastic flutter of post-buckled functionally graded panels[J]. *Chinese Journal of Theoretical and Applied Mechanics*, 2016, 48(3): 609-614. (in Chinese))
- [2] NAN Z, XIE Z, SHI JIE Z, et al. Size-dependent static bending and free vibration analysis of porous functionally graded piezoelectric nanobeams[J]. *Smart Materials and Structures*, 2020, 29(4): 045025.
- [3] VASHISHTH A K, BAREJA U. Analysis of Love waves propagation in a functionally graded porous piezoelectric composite structure[J/OL]. *Waves in Random and Complex Media*, 2022: 1-32 [2023-05-03]. <https://doi.org/10.1080/17455030.2022.2037786>.
- [4] 陈明飞,刘坤鹏,靳国永,等.面内功能梯度三角形板等几何面内振动分析[J].应用数学和力学,2020,41(2):156-170.(CHEN Mingfei, LIU Kungpeng, JIN Guoyong, et al. Isogeometric in-plane vibration analysis of functionally graded triangular plates[J]. *Applied Mathematics and Mechanics*, 2020, 41(2): 156-170. (in Chinese))
- [5] FARAJPOUR A, GHAYESH M H, FAROKHI H. A review on the mechanics of nanostructures[J]. *International Journal of Engineering Science*, 2018, 133: 231-263.
- [6] 王平远,李成,姚林泉.基于非局部应变梯度理论功能梯度纳米板的弯曲和屈曲研究[J].应用数学和力学,2021,42(1):15-26.(WANG Pingyuan, LI Cheng, YAO Linquan. Bending and buckling of functionally graded nanoplates based on the nonlocal strain gradient theory[J]. *Applied Mathematics and Mechanics*, 2021, 42(1): 15-26. (in Chinese))
- [7] ERINGEN A C. On differential equations of nonlocal elasticity and solutions of screw dislocation and surface waves[J]. *Journal of Applied Physics*, 1983, 54(9): 4703-4710.
- [8] WANG Y Q, LIANG C, ZU J W. Wave propagation in functionally graded cylindrical nanoshells based on nonlocal Flugge shell theory[J]. *The European Physical Journal Plus*, 2019, 134(5): 1-15.
- [9] ARANI A G, BARZOKI A A M, KOLAHCHI R, et al. Pasternak foundation effect on the axial and torsional waves propagation in embedded DWCNTs using nonlocal elasticity cylindrical shell theory[J]. *Journal of Mechanical Science and Technology*, 2011, 25(9): 2385-2391.
- [10] WANG Q, VARADAN V K. Application of nonlocal elastic shell theory in wave propagation analysis of carbon nanotubes[J]. *Smart Materials and Structures*, 2007, 16(1): 178-190.
- [11] KUANG Y D, HE X Q, CHEN C Y, et al. Analysis of nonlinear vibrations of double-walled carbon nanotubes conveying fluid[J]. *Computational Materials Science*, 2009, 45(4): 875-880.
- [12] MA Q, CLARKE D R. Size dependent hardness of silver single crystals[J]. *Journal of Materials Research*, 1995, 10(4): 853-863.
- [13] MC ELHANEY K W, VLASSAK J J, NIX W D. Determination of indenter tip geometry and indentation contact area for depth-sensing indentation experiments[J]. *Journal of Materials Research*, 1998, 13(5): 1300-1306.
- [14] 徐晓建,邓子辰.基于简化的应变梯度理论下Kirchhoff板模型边值问题的提法及其应用[J].应用数学和力学,2022,43(4):363-373.(XU Xiaojian, DENG Zichen. Boundary value problems of a Kirchhoff type plate model based on the simplified strain gradient elasticity and the application[J]. *Applied Mathematics and Mechanics*, 2022, 43(4): 363-373. (in Chinese))
- [15] LIM C W, ZHANG G, REDDY J N. A higher-order nonlocal elasticity and strain gradient theory and its applications in wave propagation[J]. *Journal of the Mechanics and Physics of Solids*, 2015, 78: 298-313.
- [16] MA L H, KE L L, REDDY J N, et al. Wave propagation characteristics in magneto-electro-elastic nanoshells using nonlocal strain gradient theory[J]. *Composite Structures*, 2018, 199: 10-23.
- [17] WANG P Y, LI C, LI S, et al. A variational approach for free vibrating micro-rods with classical and non-classical new boundary conditions accounting for nonlocal strengthening and temperature effects[J]. *Journal of*

- Thermal Stresses*, 2020, **43**(4): 421-439.
- [18] WANG P Y, LI C, LI S. Bending vertically and horizontally of compressive nano-rods subjected to nonlinearly distributed loads using a continuum theoretical approach[J]. *Journal of Vibration Engineering & Technologies*, 2020, **8**(6): 947-957.
- [19] SHEN J P, WANG P Y, LI C, et al. New observations on transverse dynamics of microtubules based on nonlocal strain gradient theory[J]. *Composite Structures*, 2019, **225**: 111036.
- [20] SHARIFI Z, KHORDAD R, GHARAATI A, et al. An analytical study of vibration in functionally graded piezoelectric nanoplates: nonlocal strain gradient theory[J]. *Applied Mathematics and Mechanics (English Edition)*, 2019, **40**(12): 1723-1740.
- [21] MEHRALIAN F, BENI Y T. Vibration analysis of size-dependent bimorph functionally graded piezoelectric cylindrical shell based on nonlocal strain gradient theory[J]. *Journal of the Brazilian Society of Mechanical Sciences and Engineering*, 2018, **40**(1): 27.
- [22] LIU Y F, WANG Y Q. Thermo-electro-mechanical vibrations of porous functionally graded piezoelectric nanoshells [J]. *Nanomaterials(Basel)*, 2019, **9**(2): 301.
- [23] WANG Y Q, LIU Y F, ZU J W. Analytical treatment of nonlocal vibration of multilayer functionally graded piezoelectric nanoscale shells incorporating thermal and electrical effect[J]. *The European Physical Journal Plus*, 2019, **134**(2): 1-15.
- [24] LONG H, MA H S, WEI Y G, et al. A size-dependent model for predicting the mechanical behaviors of adhesively bonded layered structures based on strain gradient elasticity[J]. *International Journal of Mechanical Sciences*, 2021, **198**: 106348.
- [25] BARATI M R, ZENKOUR A M. Electro-thermoelastic vibration of plates made of porous functionally graded piezoelectric materials under various boundary conditions[J]. *Journal of Vibration and Control*, 2016, **24**(10): 1910-1926.
- [26] ISMAIL E, RAMAZAN Ö. Thermal vibration and buckling of magneto-electro-elastic functionally graded porous nanoplates using nonlocal strain gradient elasticity[J]. *Composite Structures*, 2022, **296**: 115878.
- [27] FALEH N M, AHMED R A, FENJAN R M. On vibrations of porous FG nanoshells[J]. *International Journal of Engineering Science*, 2018, **133**: 1-14.
- [28] SAFARPOUR H, ALI GHANIZADEH S, HABIBI M. Wave propagation characteristics of a cylindrical laminated composite nanoshell in thermal environment based on the nonlocal strain gradient theory[J]. *The European Physical Journal Plus*, 2018, **133**(12): 1-17.
- [29] YANG J. *Special Topics in the Theory of Piezoelectricity*[M]. Springer Science & Business Media, 2010.